


Noise-induced symmetry breaking in a network of excitable ecological systems

Arzoo Narang,¹ Tanmoy Banerjee^{2,*} and Partha Sharathi Dutta^{1,†}

¹Department of Mathematics, Indian Institute of Technology Ropar, Rupnagar 140 001, Punjab, India

²Chaos and Complex Systems Research Laboratory, Department of Physics, University of Burdwan, Burdwan 713 104, West Bengal, India

 (Received 17 August 2022; revised 10 January 2023; accepted 27 January 2023; published 14 February 2023)

Noise-induced symmetry breaking has barely been unveiled on the ecological grounds, though its occurrence may elucidate mechanisms responsible for maintaining biodiversity and ecosystem stability. Here, for a network of excitable consumer-resource systems, we show that the interplay of network structure and noise intensity manifests a transition from homogeneous steady states to inhomogeneous steady states, resulting in noise-induced symmetry breaking. On further increasing the noise intensity, there exist asynchronous oscillations, leading to heterogeneity crucial for maintaining a system's adaptive capacity. The observed collective dynamics can be understood analytically in the framework of linear stability analysis of the corresponding deterministic system.

DOI: [10.1103/PhysRevE.107.024410](https://doi.org/10.1103/PhysRevE.107.024410)

I. INTRODUCTION

A principle finding in theoretical ecology suggests that even a simple population model can manifest a range of dynamical scenarios, from stable equilibria to cyclic oscillations, through to chaos [1]. Oscillatory dynamics has a long history, as summarized in diverse fields [2–4]. Elucidating various mechanisms behind these oscillations is a major challenge and has been of persistent interest in ecology [5]. As discussed in [6], endogenous causes are the plausible explanation for the generation of population cycles. Another well studied nonlinear phenomenon observed in dynamical systems is *excitability* [7,8]. Excitable dynamics are observed in a wide range of natural systems, which under strong perturbations can evoke large-amplitude fluctuations, before relaxing to a rest state [9]. These large-amplitude transient fluctuations can sometimes turn into sustained oscillations due to stochastic perturbations, often called noise-induced oscillations [10,11]. Here, by considering an ecological network of excitable systems, we address the following questions: Do noise-induced oscillations always directly transit from a steady state? Can other intermediate collective dynamics exist while the system shifts from a steady state to noise-induced oscillations?

Stochasticity or noise is ubiquitous in ecosystems. In recent years, extensive research on stochastic ecological systems has found that noise can lead to many novel phenomena, from population cycles to coexistence [12,13]. The persuasive role of noise on the dynamics of excitable systems is observed in many disciplines, including noise-induced oscillations [10,14], the phenomenon of coherence resonance [15,16], the occurrence of chimera states [17], and noise-enhanced synchronization in coupled excitable systems [18,19]. An intriguing phenomenon that has received less attention is noise-induced symmetry breaking (NISB). NISB affirms reduced symmetric configuration in the presence of noise, even though the underlying deterministic processes are

symmetric, thus resulting in the occurrence of multiple stable states. There is limited research on NISB [20,21], and so far, its ecological facet remains to be studied. Multiple stable solutions make it possible for populations in distinct patches and nodes to settle into different steady states, therefore minimizing the extinction risk and increasing the stability of spatial population through rescue effect [22]. The idea of spatial ecosystem functioning and species interactions goes hand in hand. Spatially separated populations, which through dispersal may synchronize, are considered necessary to understand population cycles [23]. Researchers find that large systems of interacting oscillators have promising applications in various fluctuating systems [9,24]. Further, species dispersal network structure is believed to influence the ecological dynamics strongly, as explored by recent studies [25,26]. Following those lines of thought, here we report that an interplay of network structure and noise intensity results in a transition from homogeneous steady states to inhomogeneous steady states via NISB, before turning into noise-induced asynchronous oscillations. These results are explained numerically with the help of time series, spatiotemporal plots, and phase diagrams. Further, we show that the network model's linear stability analysis can help to explain the observed dynamics.

II. MODEL OF AN ECOLOGICAL NETWORK

We consider an ecological network with N patches inhabiting resource-consumer [27] systems. The consumers in each patch are connected with other patches via a diffusive coupling, where the connectivity pattern varies from local to global. There is an additive Gaussian white noise $\xi(t)$ that affects the consumer abundance. The network model, in the presence of stochastic perturbations, is given below:

$$\epsilon \frac{dx_i}{dt} = rx_i(1 - x_i) - \frac{a^2 x_i^2}{1 + b^2 x_i^2} y_i, \quad (1a)$$

$$\frac{dy_i}{dt} = \frac{a^2 x_i^2}{1 + b^2 x_i^2} y_i - my_i + \frac{\sigma}{2P} \sum_{j=i-P}^{j=i+P} (y_j - y_i) + \sqrt{2D} \xi_i(t), \quad (1b)$$

*tbanerjee@phys.buruniv.ac.in

†Corresponding author: parthasharathi@iitpr.ac.in

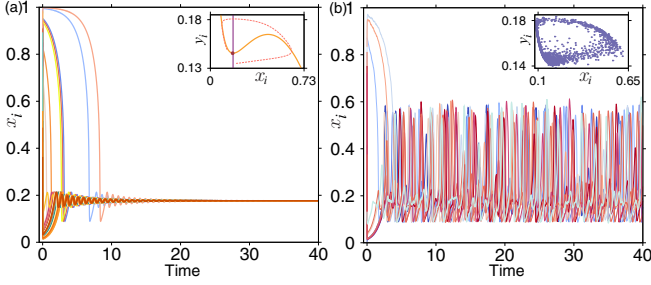


FIG. 1. Time series of the resource population (x) for the model (1) with $\sigma = 0$ and $a = 9$ (the system is in the excitable region): (a) For zero noise intensity ($D = 0$) the system settles into a steady state. Inset: nullclines of the resource (x) and the consumer (y). (b) For a nonzero noise intensity ($D = 0.000\ 05$) there exists noise-induced oscillations. Inset: stochastic cyclic attractor. Other model parameters are $r = 1$, $b = 7$, $m = 1$, $\epsilon = 0.01$, and $N = 101$.

where x_i and y_i , respectively, determine resource and consumer abundance and $i(= 1, 2, \dots, N)$ denotes the patch index (all indices are modulo N). The parameter $\epsilon > 0$ is responsible for a timescale separation between a fast resource population and a slow consumer population. The resource follows the logistic growth with an intrinsic growth rate r , and the interaction of resource and consumer is characterized by Holling’s type-III grazing with parameters a and b . m is the natural mortality of the consumer. The parameter a describes the excitability threshold of the isolated system; in particular, it determines whether the system is in the excitable

($a > 8.975$) or in the oscillatory ($a \in [7.345, 8.975]$) regime. Here, we focus on the dynamics of the resource-consumer population in the excitable regime ($a = 9$). The model assumes the movement of the consumer population between the patches, where the interaction is governed by the coupling strength σ and the parameter P controls the coupling range $s = P/N$, where $1 \leq P \leq (N - 1)/2$ for an odd number of patches. Increasing the value of P from 1 to $(N - 1)/2$ varies the network topology from local to global via non-local. Further, $\xi_i(t) \in \mathbb{R}$ is the normalized Gaussian white noise that perturbs the consumer population in each i th patch, i.e., $\langle \xi_i(t) \rangle = 0$ and $\langle \xi_i(t)\xi_j(t') \rangle = \delta_{ij}\delta(t - t')$, $\forall i, j$, and D is the noise intensity. In the excitable region, the isolated system rests in a stable steady state in the absence of noise [see Fig. 1(a)]. Inducing stochastic perturbations beyond a threshold value of the noise amplitude drives the population to produce sustained oscillations, as seen in Fig. 1(b).

III. RESULTS

The interplay of node dynamics, network topology, and noise introduced in the model (1), gives rise to distinct dynamical regimes [28]. Depending upon noise intensity D , we demonstrate four distinct space-time patterns for resource population in Fig. 2 (see Fig. 5 in the Appendix for the corresponding consumer dynamics). In the absence of noise ($D = 0$) or for a low noise intensity, all the nodes rest in the steady state, thus giving a homogeneous steady-state solution [Fig. 2(a)]. Now, in the presence of a weak noise strength, the system breaks into two subpopulations having two distinct

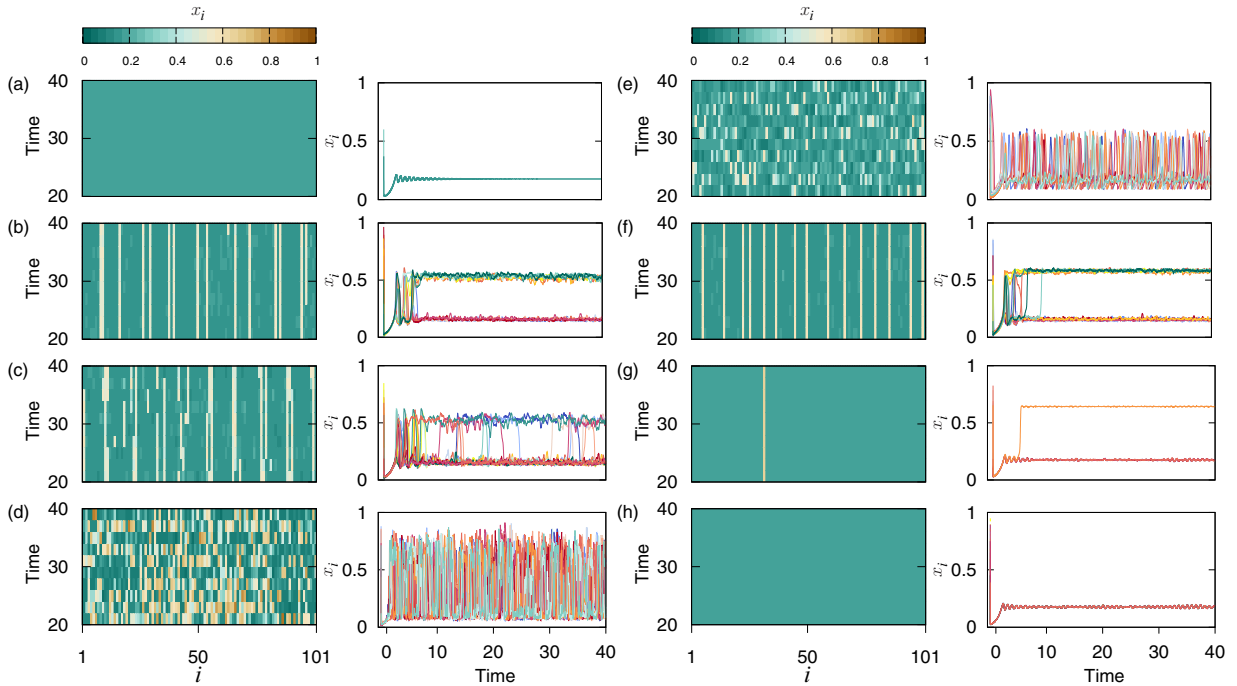


FIG. 2. (a)–(d) Space-time (left column) and corresponding time series plots (right column) of resource x_i for $P = 8$, $\sigma = 0.1$ with varying noise intensities: (a) $D = 0$; steady state, (b) $D = 0.000\ 01$; symmetry breaking, (c) $D = 0.000\ 033$; stochastic switching between two resource densities, and (d) $D = 0.005$; asynchronous oscillations. (e)–(h) Space-time (left column) and corresponding time series (right column) plots for $D = 0.000\ 01$, $\sigma = 0.6$ with varying coupling range s : (e) $s = 0.01$ (local coupling); asynchronous oscillations, (f) $s = 0.04$; symmetry breaking, (g) $s = 0.25$; symmetry breaking with most nodes settling at the lower branch, and (h) $s = 0.5$ (global coupling); steady state. Other model parameters are $r = 1$, $a = 9$, $b = 7$, $m = 1$, $\epsilon = 0.01$, and $N = 101$.

noise-induced inhomogeneous steady states. The scenario is shown in Fig. 2(b) for $D = 0.000\,01$. The time series in the right panel of Fig. 2(b) shows two distinct branches of resource densities. Interestingly, the lower branch coincides with the deterministic steady state. However, the presence of noise gives birth to an additional steady state, i.e., the upper branch. The spatiotemporal plot in the left panel of Fig. 2(b) depicts that the upper branch randomly appears in the background of the steady state of the lower branch. The presence of two steady states breaks the spatial symmetry of the system, and we get a new stationary state governed by noise-induced symmetry breaking. We find that the network exhibits stochastic switching between the two branches for an intermediate noise intensity. Figure 2(c) demonstrates this scenario for $D = 0.000\,033$. For a large noise intensity ($D = 0.005$), inhomogeneous steady states no longer exist; rather, stochastically spiking incoherent oscillations take place [see Fig. 2(d)].

Moreover, to provide an insight into the effects of network topology on the dynamics of the system, we fix the noise intensity $D = 0.000\,01$, coupling strength $\sigma = 0.6$, and vary the connectivity from local ($s = 0.01$) to global ($s = 0.5$) via nonlocal ($s = 0.03$, $s = 0.25$) coupling [see Figs. 2(e)–2(h)]. We find notable differences between dynamics with the changing network topology. Increasing the coupling range of the network not only reduces the number of solutions but also changes the dynamics from oscillatory to steady state. As observed from Fig. 2(e), local coupling favors oscillating populations with spatial incoherence, whereas increasing the coupling range shows a transition from oscillating populations [Fig. 2(e)] to inhomogeneous steady states [Figs. 2(f) and 2(g)], through to homogeneous solutions [Fig. 2(h)]. Interestingly, in the presence of nonlocal coupling, as depicted in the space-time plot in Fig. 2(f), oscillators randomly rest at the lower or the upper branch; however, with the increasing network connectivity to global coupling, all the oscillators settle at the lower branch [Fig. 2(h)], which also incites homogeneous population densities. Thus, for a fixed noise intensity D and coupling strength σ , the network model (1) experiences NISB while moving from global to local coupling.

The observed transition from oscillatory dynamics to inhomogeneous states compels us to investigate our system's qualitative behavior in these respective regimes. We analyze the features of the oscillatory region through the phase portrait in Figs. 3(a) and 3(b) for noise intensity $D = 0.005$. We observe that the density of phase points of the stochastic limit cycle attractor for one oscillator [see Fig. 3(a)] and correspondingly for all the oscillators [see Fig. 3(b)] is larger around two population densities, i.e., $x_i = 0.1$ and $x_i = 0.55$. To further elaborate on the phenomenon of symmetry breaking observed in Fig. 2, we calculate the center of mass defined as [29]

$$x_{c.m.} = \frac{1}{T} \int_0^T x_i(t) dt, \quad (2)$$

where x_i is the resource density in each i th patch, and T is taken sufficiently large. Resource population settles exactly into two branches as is characterized by two distinct values of center of mass [Fig. 3(c)], where for one part of the population $x_{c.m.} \approx 0.15$ and for the other subpopulation $x_{c.m.}$ takes

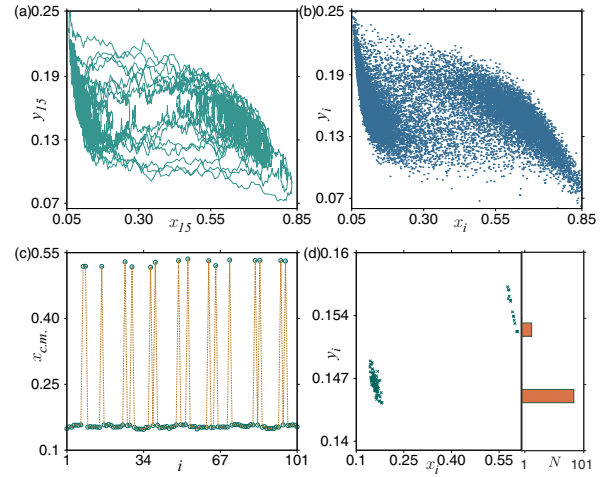


FIG. 3. Phase portraits exhibiting the long stay of attractor in the two domains around $x_i = 0.1$ and $x_i = 0.55$ for (a) one oscillator (15th node) and (b) all the oscillators, at noise intensity $D = 0.005$. (c) Center of mass ($x_{c.m.}$) and (d) phase portrait at a particular time along with density distribution of y_i corresponding to NISB for nonlocal coupling ($P = 8$) at noise intensity $D = 0.000\,01$. The histogram in the right panel of (d) represents the number of oscillators in either of the two states. Other model parameters are $r = 1$, $a = 9$, $b = 7$, $m = 1$, $\epsilon = 0.01$, $\sigma = 0.1$, and $N = 101$.

the value around 0.5, therefore exhibiting two nonuniform states. A relevant observation illustrated in the phase space [Fig. 3(d)] suggests an underlying mechanism for symmetry breaking, specifically NISB, clearly indicating the coexistence of two steady states in the network. We observe that wide distributions show up for two density values (≈ 0.15 and ≈ 0.5), thus settling the system solely around these two states.

To gain a comprehensive view of the spatiotemporal dynamics in the network, we compute phase diagrams in the (s, D) and (s, σ) parameter planes [see Figs. 4(a) and 4(b), respectively]. Keeping the value of coupling strength σ fixed to 0.1, we vary s and D in Fig. 4(a). For stronger noise intensity D , in the entire range of s , the system resides in the asynchronous oscillatory regime. For weaker values of D , we observe either asynchronous oscillations or NISB, along with a region of stochastic switching, depending upon the coupling range s . NISB occurs for a certain threshold value of $s > 0.07$, i.e., when the coupling is nonlocal with around eight nodes connected and persists up to $s = 0.5$ (globally coupled). However, local coupling ($s = 0.01$) and less connected nodes (up to six) maintain the oscillatory behavior. Moreover, a narrow zone of stochastic switching is observed between these two regimes. In Fig. 4(b), we explore the interplay of s and σ , with the value of D being fixed to 0.000 01. The oscillatory region observed for a large number of connected nodes $s = 0.21$, narrows down to $s = 0.02$ with increasing coupling value σ , clearly determining the persisting oscillatory pattern for local coupling in the whole range of σ . Moreover, for a large value of σ (≈ 0.53), a transition from oscillations to NISB via stochastic switching takes place for a lower coupling range. In contrast, with decreasing coupling strength, more connected nodes are required for the transition. In the direction of global coupling, beyond a threshold value of σ , the system traverses a synchronous steady state [homogeneous steady state (HSS)].

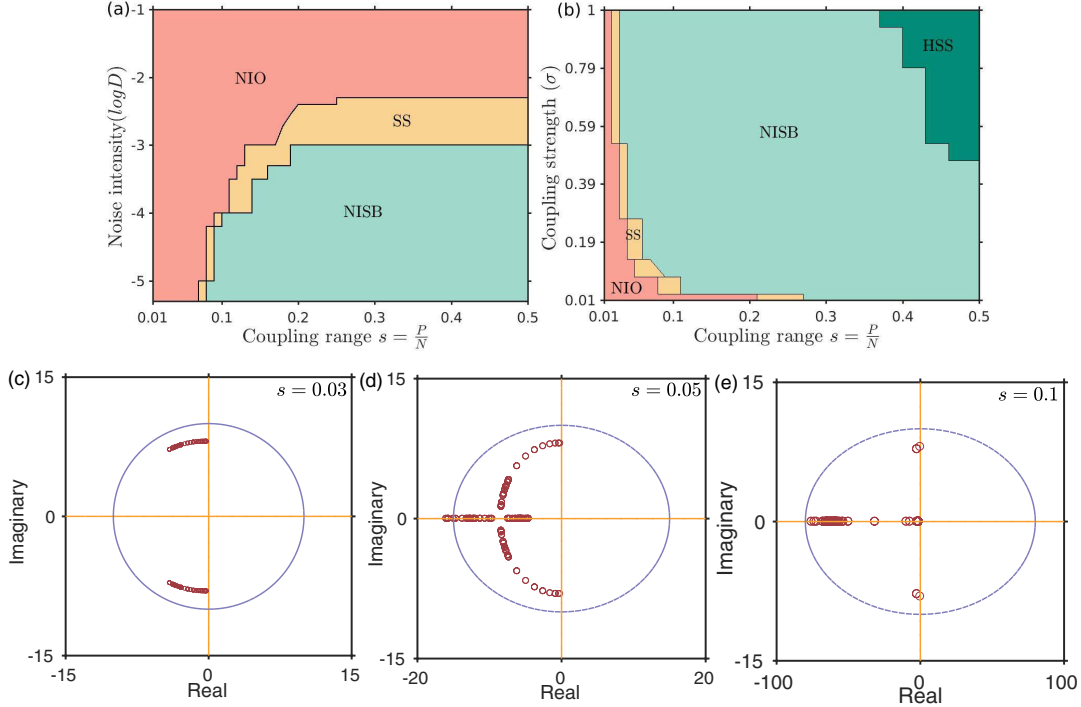


FIG. 4. Phase diagrams in the (a) (s, D) plane for $\sigma = 0.1$ and (b) (s, σ) plane for $D = 0.00001$, where NIO: noise-induced oscillations, SS: stochastic switching, NISB: noise-induced symmetry breaking, and HSS: homogeneous steady state. (c)–(e) Distribution of the eigenvalues for different values of s for $\sigma = 0.6$ and $D = 0$. Other model parameters are the same as in Fig. 2.

Our results can have significant implications for understanding the positive effects of noise on species diversity. Metapopulations are essential as it supports the persistence of many species under the events of local extinctions and recolonization. Understanding the ecological effects of population cycles on ecosystem processes is also challenging. Studies [30–32] suggest that cycles promote the coexistence of several consumers competing for shared resources. The work by Eveleigh *et al.* [33] shows that cyclic species can enhance biodiversity through the “bird-feeder effect.” Therefore, oscillatory dynamics may significantly contribute towards biodiversity maintenance [34]. Further, ecologists predict that large population fluctuations could shift communities from one state to another. The presence of alternative stable equilibria allows populations in different patches to settle in any

stable states depending upon the initial conditions. Thus there is no spatial synchronization, which impedes extinction [22].

The noise intensity D considered for our analysis is in the order of 10^{-5} (see Fig. 2). Thus, a careful investigation of the model (1) in the deterministic limit can give an insight to explain the observed dynamics. Therefore, considering the deterministic framework, i.e., $D = 0$ in (1), we carry the linear stability analysis. We calculate eigenvalues of the linearized system using the equilibrium points based upon the changing network topology [35]. Let $(x^*, y^*) = (x_1^*, y_1^*, x_2^*, y_2^*, \dots, x_N^*, y_N^*)$ be a nontrivial equilibrium point of the system (1) when $D = 0$. Linearization of the deterministic system in the neighborhood of the equilibrium point (x^*, y^*) yields the following block-structured matrix:

$$J = \begin{bmatrix} J_1(x_1^*, y_1^*) - \text{diag}\{0, 2P\} & \vdots & \text{diag}\{0, m_j\} & \vdots & \dots & \vdots & \text{diag}\{0, m_j\} \\ \text{diag}\{0, m_j\} & \vdots & J_2(x_2^*, y_2^*) - \text{diag}\{0, 2P\} & \vdots & \text{diag}\{0, m_j\} & \vdots & \dots \\ \vdots & \vdots & \vdots & \vdots & \vdots & \vdots & \vdots \\ \text{diag}\{0, m_j\} & \vdots & \text{diag}\{0, m_j\} & \vdots & \dots & \vdots & J_N(x_N^*, y_N^*) - \text{diag}\{0, 2P\} \end{bmatrix},$$

where J_i is the Jacobian of the isolated i th patch at an equilibrium point (x_i^*, y_i^*) ($i = 1, 2, \dots, N$) given as

$$J_i = \begin{bmatrix} j_{11}^i & j_{12}^i \\ j_{21}^i & j_{22}^i \end{bmatrix},$$

with $j_{11}^i = \frac{1}{\epsilon} - \frac{2x_i^*}{\epsilon} - \frac{1}{\epsilon} \frac{2a^2 x_i^* y_i^*}{1+b^2 x_i^{*2}}$, $j_{12}^i = -\frac{1}{\epsilon} \frac{a^2 x_i^{*2}}{1+b^2 x_i^{*2}}$, $j_{21}^i = \frac{2a^2 x_i^{*2} y_i^*}{(1+b^2 x_i^{*2})^2}$, and $j_{22}^i = \frac{a^2 x_i^{*2}}{1+b^2 x_i^{*2}} - 1$. Further, $m_j = 1$ if the i th and j th nodes are connected, and $m_j = 0$ otherwise.

The coupling strength $\sigma = 0.6$ and noise intensity $D = 0.00001$ manifest four distinct regimes based upon the value of s , as can be seen in Fig. 4(b). The transition from oscillatory dynamics to NISB via stochastic switching (SS) occurs for $s = 0.05$, further traversing HSS around $s = 0.41$. Here we intend to investigate whether the node dynamics and network structure determine the dominant pattern of NISB in the limiting value of D tending to 0. Figures 4(c)–4(e) show the distribution of eigenvalues with varying coupling range s .

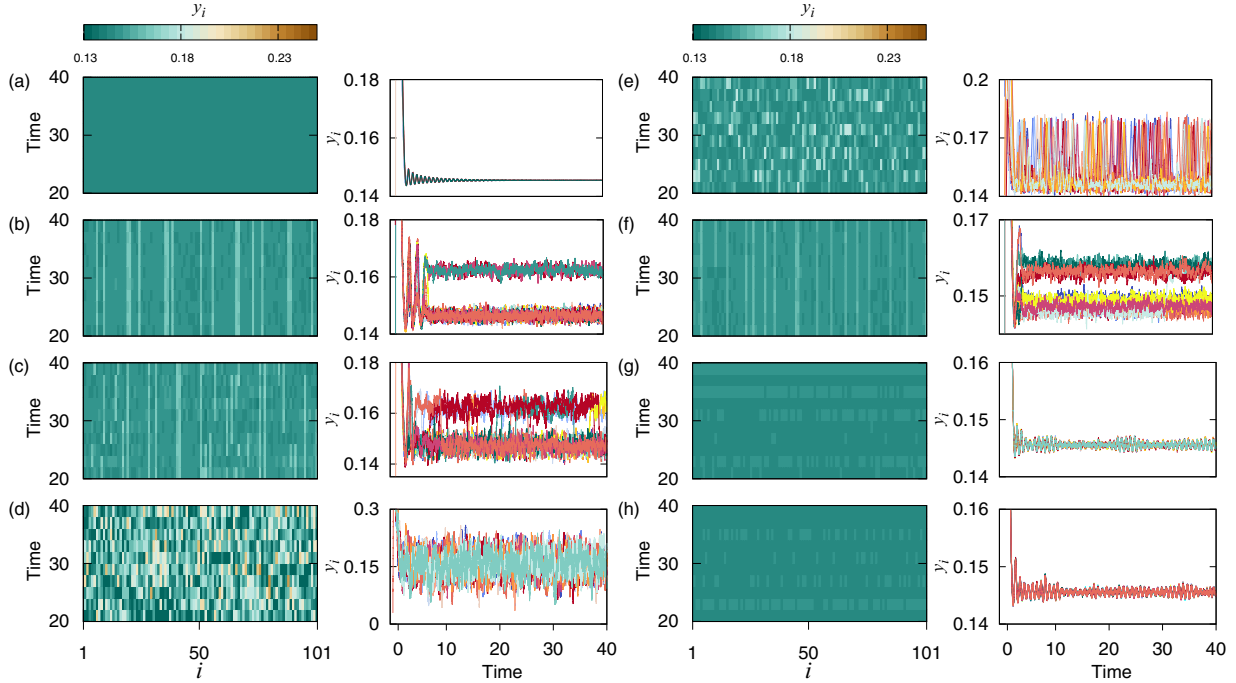


FIG. 5. (a)–(d) Space-time (left column) and corresponding time series plots (right column) of consumer y_i for $P = 8$, $\sigma = 0.1$ with varying noise intensities: (a) $D = 0$; steady state, (b) $D = 0.00001$; symmetry breaking, (c) $D = 0.000033$; stochastic switching between two consumer densities, and (d) $D = 0.005$; frequent spiking. (e)–(h) Space-time (left column) and corresponding time series (right column) plots for $D = 0.00001$, $\sigma = 0.6$ with varying coupling range s : (e) $s = 0.01$ (local coupling); asynchronous oscillations, (f) $s = 0.04$; symmetry breaking, (g) $s = 0.25$; most nodes settling at the lower branch, and (h) $s = 0.5$ (global coupling); steady state. Other model parameters are $r = 1$, $a = 9$, $b = 7$, $m = 1$, $\epsilon = 0.01$, and $N = 101$.

We observe complex conjugate eigenvalues (λ_i) for s ranging from 0.01 to 0.04 as shown for $s = 0.03$ in Fig. 4(c). It is ascertained from Fig. 4(c) that the fixed point obtained at $D = 0$ for $s = 0.03$ is a stable spiral since $\text{Real}(\lambda_i) < 0 \forall i$. However, as analyzed from Fig. 4(b) for the same coupling range ($s = 0.03$), the presence of noise in the system results in the occurrence of oscillations or SS. A recent study [36] demonstrated the impact of additive noise on networks, tuning their spectral properties. The work showed that increasing noise intensity could coerce the eigenvalues to cross the imaginary axis. Moreover, oscillations in stochastic excitable systems are known to occur due to noisy perturbations [14]. Noise-driven excitable systems possess noise-induced eigenfrequency, and thus can exhibit stochastic oscillations. The work by Hidalgo *et al.* [37] describes the phenomenon of “stochastic amplification of fluctuations.” The mechanism is associated with the resonance amplification of some frequencies when the corresponding steady-state equilibrium of the deterministic system has complex eigenvalues. Therefore, we infer that the transition from a steady state ($D = 0$) to an oscillatory state or a region of SS ($D \neq 0$) in our work is due to stochastic amplification of fluctuations and the impact of noise on the eigenvalue spectrum that resulted in destabilizing the equilibrium point by crossing the imaginary axis, and hence the occurrence of Hopf bifurcation. Moving further to $s = 0.05$, we observe the emergence of a few real eigenvalues [see Fig. 4(d)], which also eventually tend towards 0 with increasing coupling range ($s = 0.1$), as observed from Fig. 4(e). We also notice that the number of real eigenvalues

increases in a passage of global coupling. Thus, we infer that the presence of noise in the network (1) can lead the real eigenvalues to cross the origin, henceforth inducing NISB via a pitchfork bifurcation.

IV. CONCLUSION

In conclusion, we have shown that an ecological network of identical excitable systems can be driven out of the resting state leading to different collective dynamics, including regimes of heterogeneous steady states and asynchronous oscillatory states, mediated by noise intensity and network topology. For nonlocal coupling and adequately tuning the noise intensity, we achieve an oscillatory regime due to the resonance effect [11] or a region of inhomogeneous steady states (NISB). Further, by keeping the noise intensity fixed while changing the coupling range from local to global, we identify a transition from an oscillatory domain to a region HSS through NISB. Although the oscillatory and inhomogeneous steady states promote species’ sustainability, the emergence of HSS while traversing towards global coupling inhibits biodiversity [26]. Our results are robust across a large region in the parameter space, as demonstrated via phase diagrams. Therefore, our findings could be important for understanding the mechanisms responsible for upholding biodiversity and ecosystem stability. Finally, deriving the Fokker-Planck equation of stochastic ecological networks for the analytical tractability of the observed collective dynamics is an important future direction.

ACKNOWLEDGMENTS

P.S.D. acknowledges financial support from the Science & Engineering Research Board (SERB), Government of India (Grant No. MTR/2021/000148).

APPENDIX: STOCHASTIC CONSUMER DYNAMICS

In Fig. 5, we demonstrate the effect of noise intensity and network topology on consumer (y) dynamics (corresponding to Fig. 2). For a fixed coupling range $P = 8$ and in the absence of noise ($D = 0$) we observe that all the nodes rest in the steady state [Fig. 5(a)]. Adding noise into the system ($D > 0$), although with weak intensity, results in two inhomogeneous steady solutions, as shown in Fig. 5(b) for $D = 0.00001$. However, due to the low population density maintained by consumers, the upper and the lower steady-

state branches do not have a large difference, as was in the case of resource (x) densities [see Fig. 2(b)]. Further, increasing noise intensity results in the switching between the two branches of consumer densities [Fig. 5(c)]. For a large noise intensity ($D = 0.005$), frequent spiking is noticed [see Fig. 5(d)].

Moving ahead, for a fixed noise intensity $D = 0.00001$ and for local coupling ($s = 0.01$), we observe oscillating dynamics of the consumer population from Fig. 5(e). Increasing the coupling range results in symmetry breaking as is exhibited by the consumer population settling in the two branches [see Fig. 5(f)], where the densities of the upper and the lower branches are not very significantly apart. Therefore, any further increase in connectivity leads to the collision of the two states, thus resulting in a single steady-state solution [Figs. 5(g) and 5(h)].

-
- [1] R. M. May, *Science* **186**, 645 (1974).
 [2] E. Benincà, B. Ballantine, S. P. Ellner, and J. Huisman, *Proc. Natl. Acad. Sci. USA* **112**, 6389 (2015).
 [3] C. S. Elton, *J. Exp. Biol.* **2**, 119 (1924).
 [4] P. Rohani, D. J. Earn, and B. T. Grenfell, *Science* **286**, 968 (1999).
 [5] P. Turchin and S. P. Ellner, *Ecology* **81**, 3099 (2000).
 [6] S. E. Kingsland, *Modeling Nature* (University of Chicago Press, Chicago, 1995).
 [7] E. Meron, *Phys. Rep.* **218**, 1 (1992).
 [8] P. Olla, *Phys. Rev. E* **87**, 012712 (2013).
 [9] E. M. Izhikevich, *Dynamical Systems in Neuroscience* (MIT, Cambridge, MA, 2007).
 [10] W. H. Nasse, C. A. Del Negro, and P. C. Bressloff, *Phys. Rev. Lett.* **101**, 088101 (2008).
 [11] E. Benincà, V. Dakos, E. H. Van Nes, J. Huisman, and M. Scheffer, *American Naturalist* **178**, E85 (2011).
 [12] P. Moran, *Aust. J. Zool.* **1**, 163 (1953).
 [13] N. C. Stenseth, O. N. Bjørnstad, and T. Saitoh, *Proc. R. Soc. London, Ser. B* **263**, 1117 (1996).
 [14] U. Hillenbrand, *Phys. Rev. E* **66**, 021909 (2002).
 [15] J. M. Buldú, J. García-Ojalvo, C. R. Mirasso, M. C. Torrent, and J. M. Sancho, *Phys. Rev. E* **64**, 051109 (2001).
 [16] A. Ganopolski and S. Rahmstorf, *Phys. Rev. Lett.* **88**, 038501 (2002).
 [17] N. Semenova, A. Zakharova, V. Anishchenko, and E. Schöll, *Phys. Rev. Lett.* **117**, 014102 (2016).
 [18] A. Neiman, L. Schimansky-Geier, A. Cornell-Bell, and F. Moss, *Phys. Rev. Lett.* **83**, 4896 (1999).
 [19] C. D. E. Boschi, E. Louis, and G. Ortega, *Phys. Rev. E* **65**, 012901 (2001).
 [20] T. J. Kobayashi, *Phys. Rev. Lett.* **106**, 228101 (2011).
 [21] F. Jafarpour, T. Biancalani, and N. Goldenfeld, *Phys. Rev. E* **95**, 032407 (2017).
 [22] R. E. Amritkar and G. Rangarajan, *Phys. Rev. Lett.* **96**, 258102 (2006).
 [23] E. Ranta, V. Kaitala, and P. Lundberg, *Science* **278**, 1621 (1997).
 [24] B. Blasius, A. Huppert, and L. Stone, *Nature (London)* **399**, 354 (1999).
 [25] M. D. Holland and A. Hastings, *Nature (London)* **456**, 792 (2008).
 [26] A. Gupta, T. Banerjee, and P. S. Dutta, *Phys. Rev. E* **96**, 042202 (2017).
 [27] J. Truscott and J. Brindley, *Bull. Math. Biol.* **56**, 981 (1994).
 [28] We have numerically solved the stochastic model (1) using the Euler-Maruyama method with integration step size 10^{-3} , and initial conditions are randomly generated from the uniform distribution on the interval $(0,1)$.
 [29] A. Zakharova, M. Kapeller, and E. Schöll, *Phys. Rev. Lett.* **112**, 154101 (2014).
 [30] R. A. Armstrong and R. McGehee, *American Naturalist* **115**, 151 (1980).
 [31] P. S. Dutta, B. W. Kooi, and U. Feudel, *Theor. Ecol.* **7**, 407 (2014).
 [32] P. S. Dutta, B. W. Kooi, and U. Feudel, *J. Theor. Biol.* **417**, 28 (2017).
 [33] E. S. Eveleigh, K. S. McCann, P. C. McCarthy, S. J. Pollock, C. J. Lucarotti, B. Morin, G. A. McDougall, D. B. Strongman, J. T. Huber, J. Umbanhowar *et al.*, *Proc. Natl. Acad. Sci. USA* **104**, 16976 (2007).
 [34] P. Chesson, *Annu. Rev. Ecol. Syst.* **31**, 343 (2000).
 [35] D. O. Logofet, *Matrices and Graphs: Stability Problems in Mathematical Ecology* (CRC, Boca Raton, FL, 2018).
 [36] A. Hutt, A. Mierau, and J. Lefebvre, *PLoS One* **11**, e0161488 (2016).
 [37] J. Hidalgo, L. F. Seoane, J. M. Cortès, and M. A. Munoz, *PLoS One* **7**, e40710 (2012).